JOURNAL OF MATERIALS SCIENCE 32 (1997) 4847–4855

Massive transformation in an Fe–Cu alloy

N. M. HWANG
Korea Research Institute of Standards and Science, PO Box 102, Daedok Science Town, Daejon 305-600, South Korea

D. Y. YOON
Korea Advanced Institute of Science and Technology, 373-1 Gusungdong Yusunggu, Daejon 305-701, South Korea

A typical microstructure characteristic of massive transformation such as ''boundary crossing'' and ''irregular and jagged boundaries'' was observed in an Fe–Cu alloy after water quenching and after cooling at a rate of $0.1\,^{\circ}C\,s^{-1}$, which is far slower than that specified previously for the massive reaction. On the basis of the microstructure evolution and differential thermal analysis (DTA), it is shown that the massive transformation from γ to α occurs during isothermal holding at 810 °C but not at 830 °C. During isothermal holding at 810 °C, the composition of the supercooled γ phase is shifted into the metastable α one-phase region with the continuous precipitation of the Cu-rich ε phase. These experimental results imply that the supercooling into the one-phase region is a sufficient condition for the massive reaction to operate as long as the supercooled temperature is high enough to allow the thermally activated atomic jumps across the phase boundary.

1. Introduction

Since the massive transformation was first observed in a Cu–Zn alloy by Phillips [1] in 1930, it has been extensively investigated by Massalski and his colleagues [2–5]. Growth of the product phase in the massive transformation proceeds by the movement of the incoherent boundary without accompanying the composition change. The characteristic microstructural feature is irregular boundaries mixed with jagged and curved boundaries [2–5]. Another feature is the growth of the product phase across the grain boundary of the parent phase [5], and this "boundary crossing" has been used as a microstructural criterion for distinguishing the massive transformation from others such as an equilibrium transformation and a martensitic transformation. However, there remain some disagreements about this phenomenon, one of which is on the cooling rate required for the massive transformation to operate [4, 6–9]. Because of this disagreement, there is some ambiguity about the classification of the massive transformation in relation to the other transformations.

Recently, we [10] proposed that the cooling rate for the massive transformation need not be so high as had been claimed before based on the three-zone behaviour [4]. The purpose of this paper is to clarify the massive transformation by showing the extreme case of the massive transformation in the Fe–Cu alloy, which can take place at an extremely slow cooling rate and even during the isothermal holding.

The Fe–Cu alloy is special in studying the massive transformation. The alloy [11] shows a eutectoid reaction at about 850 °C, where the γ phase is decomposed into the Fe-rich α phase and the Cu-rich ε phase. The precipitation of ε from γ takes place by spinodal reaction [12], which makes the transformation from γ to α unusual. In contrast with the usual eutectoid decomposition by the lamella reaction, where the composition of the parent matrix changes discontinuously at the transformation front, the composition of the γ matrix changes continuously with the precipitation of ε. Cu is continuously depleted from the γ matrix with the precipitation of Cu-rich ε and finally the composition of the γ matrix falls into the metastable α one-phase region during cooling, and the composition-invariant $\gamma \rightarrow \alpha$ transformation can take place. This mode of transformation takes place even during the isothermal holding below the eutectoid temperature.

The Fe–Cu specimen was prepared by liquid-phase sintering, where the Fe-rich spherical solid grains are dispersed in the liquid matrix. Contacted grains have grain boundaries between them along the dihedral junction. The growth of the α phase into these grain boundaries can be easily identified.

2. Experimental procedure

Electrolytic Cu powder from US Bronze Powders Inc. with the purity specified to be 99.5% was used. Fe powder, which is a product from Teledyne Co. produced by the carbonyl process with the purity specified to be 99.5%, was used. Two compositions, Fe–50 wt% Cu and Fe–20 wt% Cu, were chosen for

0022–2461

the microstructural observations. With these compositions, appreciable amounts of liquid phase exist at the sintering temperature of 1150 °C. Another composition, Fe–10 wt% Cu, was chosen for the differential thermal analysis (DTA). The Fe–10 wt% Cu composition is close to that of Fe-rich grains at 1150 °C.

The mixed powder was compacted under 30 MPa into pellets of cylindrical shape 10 mm in diameter and 8–10 mm in height. The compacts were mostly sintered at 1150 °C for 24 h in a horizontal tube furnace under flowing hydrogen. The cooling rate was varied by controlling the speed of pulling the specimen out of the tube furnace. For water quenching, the alumina rod carrying the specimen was pulled out of the furnace manually and the specimen was dropped into the water. The temperature change from 1150 to 830 or 810 °C for the Fe–20 wt% Cu specimens was achieved using the temperature controller of the furnace with the specimen placed in the uniform zone. The time taken for the temperature change was about 1 h.

DTA measurements were carried out under a reducing atmosphere consisting of a gas mixture of 5.5% hydrogen and 94.5% nitrogen. The powder mixtures of Fe–10 wt% Cu were heated to 1150 °C and held for 3 h for sintering. Three specimens were cooled to 830 °C, 810 °C and 800 °C, respectively and held isothermally for 10–12 h before cooling to room temperature. The samples were cooled from 1150 to 20 °C above the holding temperature at 15 °C min^{-1} and then finally approached the holding temperature at 5 °C min^{-1}. This two-step cooling was aimed at preventing the furnace temperature from overshooting below the final isothermal holding temperature.

For microstructure observation by optical microscopy (OM) and scanning electron microscopy (SEM), the polished surface of the specimen was etched with Nital solution which revealed the α grain boundaries and contrast between the α grains.

3. Results and discussion

3.1. Effect of the cooling rate

Figs 1a and b show the microstructures of the Fe–50 wt% Cu specimens which were sintered for 24 h at 1150 °C and cooled to room temperature by water quenching and at 0.1 °C s^{-1}, respectively. The spherical grains are the Fe-rich solid solution, containing about 10 wt% Cu at 1150 °C. These grains had been γ during sintering at 1150 °C and transformed to α during cooling. The white matrix was a Cu-rich phase, which was liquid at 1150 °C and solidified during cooling. In Fig. 1b, the dark fine Fe-rich precipitates are observed on this white copper-rich matrix. These precipitates had formed in the solid state owing to the slow cooling.

Each spherical Fe-rich grain had been a single crystal of γ during liquid-phase sintering but became a polycrystal of α after cooling. The γ grain boundaries had existed along the dihedral junctions of the spherical grains in contact. Some α grains appear dark while others bright because of the orientation dependence of etching; the α grain whose cubic axis lies vertical to the surface is hard to etch by the Nital solution [13]. The grain boundaries of α are also revealed by the preferential etching.

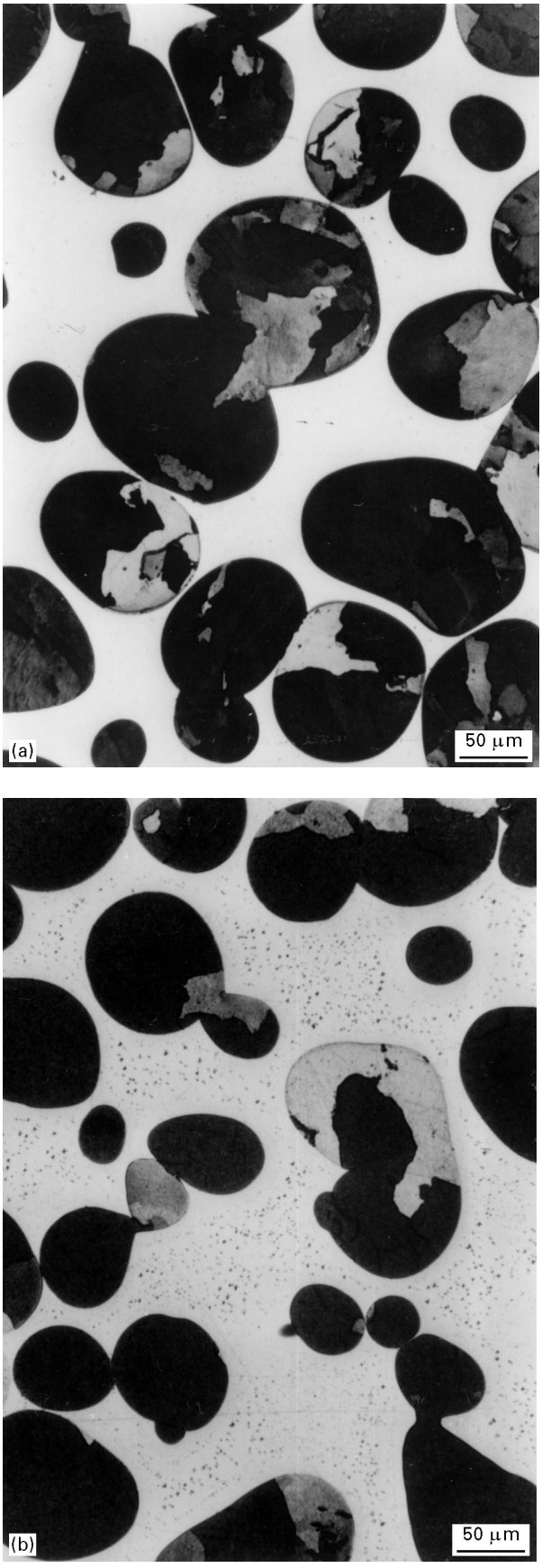

Figure 1 Microstructures of the Fe–50 wt% Cu specimens sintered at 1150 °C for 24 h and then (a) water quenched and (b) cooled at 0.1 °C s^{-1}.

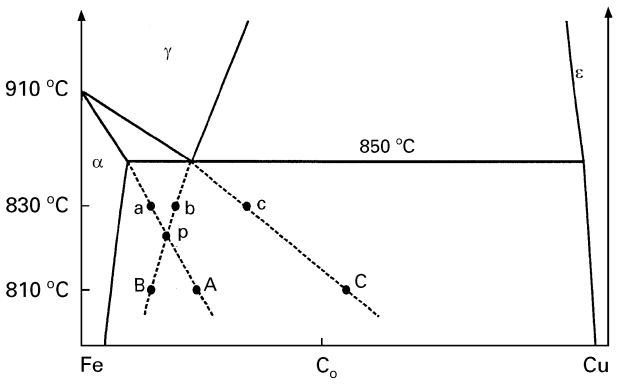

Figure 2 Schematic phase diagram of the Fe–Cu alloy showing the metastable extensions in the Fe-rich region.

The microstructures in Figs 1a and b show basically the same features; some α grains grew across the grain boundaries of the prior γ grains, and the grain boundaries of the α phase are very irregular. These microstructural features are unique to the massive transformation. Although the cooling rate was markedly different between the two specimens, the morphological features are almost the same except that α grain boundaries in Fig. 1a are slightly more jagged than those in Fig. 1b.

The transformation from γ to α in Fig. 1 can be understood by considering the metastable extensions of α–(α + γ), γ–(γ + ε) and (α + γ)–γ boundaries in the Fe–Cu phase diagram as drawn schematically in Fig. 2. The eutectoid composition of γ is Fe–2.7 at% Cu, which is in equilibrium with the Fe–1.9 at% Cu composition of the α and the Fe–98.7 at% Cu composition of the ε [11]. In the schematic phase diagram of Fig. 2, the Fe-rich region is enlarged in order to focus on the metastable equilibrium for the $\gamma \rightarrow \alpha$ transformation. The metastable extensions of α–(α + γ), γ–(γ + ε) and (α + γ)–γ are represented by the broken lines αA, bB and cC, respectively. If the initial composition of γ at the sintering temperature is C_0 in Fig. 2, the composition of γ will shift to a Fe-rich composition during cooling by the precipitation of the proeutectoid ε.

Even when the specimen is cooled below the eutectoid temperature, the precipitation of the ε phase will continue and the composition of γ will continue to shift to the Fe-rich region. Supersaturation of copper in the γ matrix comes mainly from three factors: firstly the supercooling effect, secondly the strain energy of the coherent ε precipitates and thirdly the capillary effect of the ε precipitates. The supercooling effect would be small because the nucleation barrier is negligible for the spinodal precipitation. The strain energy and the capillary effect of the ε precipitates, which affect the metastable equilibrium between γ and ε, will be reduced by their coarsening. Since it takes time for coarsening, the slower the cooling rate, the richer in Fe is the composition of γ. Thus, the slower the cooling rate, the higher the temperature at which the γ matrix falls into the metastable α one-phase region becomes. This temperature is determined by the intersection between the line *aA* in Fig. 2 and the composition of the remaining γ matrix.

Once the composition of γ falls below the line aA in Fig. 2, the transformation from γ to α does not require any composition change, only a lattice change from face-centred cubic to body-centred cubic is required. Since the temperature is high enough, this $\gamma \rightarrow \alpha$ transformation can be a composition invariant and thermally activated process. Because of the spinodal precipitation of ε, it seems that this mode of $\gamma \rightarrow \alpha$ transformation will take place almost independently of the cooling rate. For the rapid cooling of water quenching chosen in the specimen of Fig. 1a, the composition of γ would intersect the line aA at a relatively low temperature. For extremely slow cooling as low as $0.1\ ^{\circ}C\ s^{-1}$ chosen in the specimen of Fig. 1b, the composition of γ would intersect the line aA at a relatively high temperature. We confirmed by the thermal arrest measurement that the $\gamma \rightarrow \alpha$ transformation took place at a higher temperature with decreasing cooling rate. For a Fe–10 wt% Cu specimen, the thermal arrests were found at about 750 °C and 810 °C at cooling rates of $1\ ^{\circ}C\ s^{-1}$ and $0.1\ ^{\circ}C\ s^{-1}$, respectively.

Since the $\gamma \rightarrow \alpha$ transformation does not require a composition change, the growth will be interface controlled. The irregular α grain boundaries in Figs 1a and b indicate that the growth rate of the α phase was irregular along the growing front of the interphase. This irregular growth rate seems to come from the nature of the interface-controlled growth; in the interface-controlled growth, the growth rate of each segment of the interphase will depend sensitively on the local situation such as the inclination angle and the build-up or removal of the latent heat evolved by the transformation. This mode of growth is in contrast with the diffusion-controlled growth for the transformation involving the composition change, where the evolved interphase boundaries are not normally so irregular.

On the other hand, the $\gamma \rightarrow \alpha$ transformation is a serial process of nucleation and growth. In this interface-controlled growth, the growth rate would be relatively higher than the nucleation rate. Thus, the overall process will be nucleation controlled. The microstructure evolved by the nucleation-controlled process would be quite different from that by the growth-controlled process. The nucleation will take place at the site of the low nucleation barrier. For example, with the extremely slow cooling rate of $0.1\ ^{\circ}C\ s^{-1}$ chosen in the specimen of Fig. 1b, the supercooling would be small and nucleation is expected at the limited sites of the lowest nucleation barrier such as four grain corners. Once the nucleation starts, the growth rate is very high and the growing front can move into another grain, which was not occupied by the new phase because of the relatively low nucleation rate. Then, the growing front of the new phase can grow across the grain boundary of the parent phase even at the slow cooling rate, leading to the microstructure of Fig. 1b.

It should be noted that the grain boundary of the parent phase does not provide any barrier to the growth by the thermally activated process. We believe that, in the thermally activated process, the growth across the grain boundary of the parent phase is not

related to the high cooling rate, to the orientation relationship nor to the nature of the coherent and the incoherent phase boundaries; the boundary crossing comes from the nature of the nucleation-controlled process.

In the growth-controlled transformation, however, the grain boundary will be occupied by the new phase, which was nucleated before the growing front reaches the grain boundary. Thus, the growth across the grain boundary of the parent phase cannot be normally observed. Martensitic transformation is also known to be nucleation-controlled but athermal; it proceeds by the movement of the glissile plane, which has the orientation relationship with the parent phase and the boundary crossing is not expected.

We suggest that the irregular boundaries and the boundary crossing in Figs 1a and b should be related to the nature of the interface-controlled growth and the nature of the nucleation-controlled process, respectively. The microstructural features of Figs 1a and b are the same as the morphological characteristic of the massive transformation such as the irregular boundaries and the boundary crossing. Thus, the $\gamma \rightarrow \alpha$ transformation of Figs 1a and b, which is the thermally activated and composition-invariant process, should be classified as the massive transformation.

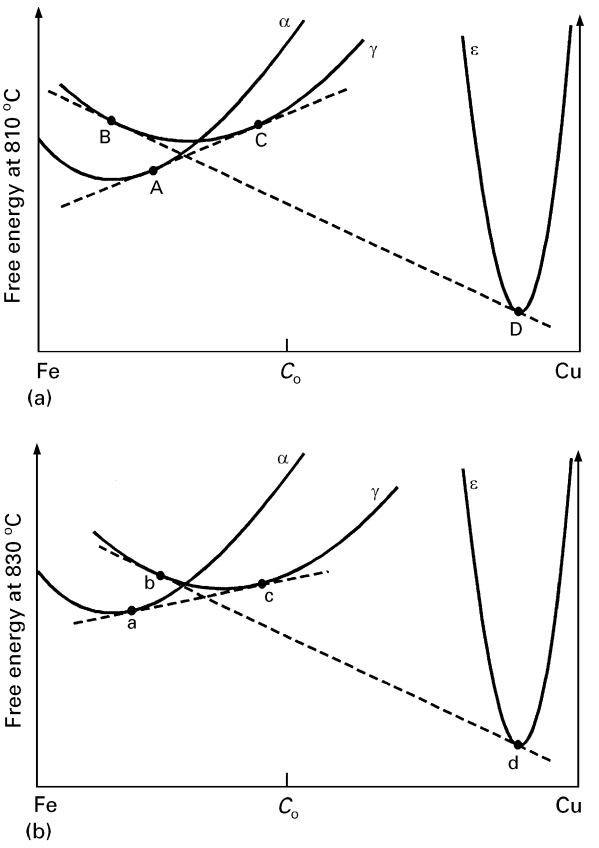

Figure 3 Schematic curves of the free energy versus composition showing the metastable equilibriums (a) at 810 °C and (b) at 830 °C.

3.2. Isothermal $\gamma \rightarrow \alpha$ transformation

Even when the γ phase supercooled below the eutectoid temperature is held isothermally, its composition will shift to the Fe-rich side by the precipitation of ε and can fall below the line of aA of Fig. 2, leading to the isothermal composition-invariant $\gamma \rightarrow \alpha$ transformation. The limit of the copper depletion in the γ matrix by the precipitation of ε is the metastable extension of the γ–$(\gamma + \varepsilon)$ boundary shown in Fig. 2. The intersection between the γ–$(\gamma + \varepsilon)$ and the α–$(\alpha + \gamma)$ boundaries is calculated to be 823 °C from the thermodynamic data of the Fe–Cu system [14] and is indicated as p in Fig. 2. Thus, below 823 °C the isothermal holding can deplete copper in the γ matrix by the precipitation of ε and the composition of the remaining γ matrix may fall into the metastable α one-phase region. On the other hand, above 823 °C the isothermal holding cannot make the composition of the γ phase fall into the metastable α one-phase region.

The curves of Gibbs free energy versus composition at 810 °C and at 830 °C are shown schematically in Figs 3a and b, respectively. The broken lines AC and BD represent the metastable equilibrium between α and γ and between γ and ε, respectively, at 810 °C. The points A, B and C at 810 °C and a, b and c at 830 °C in Fig. 2 correspond to those in Fig. 3a and in Fig. 3b, respectively. At 810 °C, the composition of γ changes with the precipitation of ε from its initial composition C_0 to the limit, B, which is determined by the common tangent of γ and ε. Since the composition of B is outside the common tangent of α and γ, i.e. in the metastable α one-phase region, the composition-invariant transformation from the remaining γ to α is possible. At 830 °C, however, the composition of γ changes from its initial composition to the limit, b, which is inside the common tangent of α and γ, i.e. in the metastable $\alpha + \gamma$ two-phase region. In this metastable $\alpha + \gamma$ region, the composition-invariant transformation from γ to α during holding is not expected.

In order to test this possibility, we prepared two specimens: one for holding at 810 °C and the other for holding at 830 °C. Two Fe–20 wt% Cu powder compacts were sintered at 1150 °C for 12 h; then one was cooled to 810 °C and the other to 830 °C and held for 48 hours before being cooled to room temperature. The microstructures shown by OM for the specimens isothermally held at 810 °C and 830 °C are shown in Figs 4a and b, respectively. The microstructural features of the massive transformation such as the boundary crossing and the irregular boundaries are shown within the Fe-rich particles of both Fig. 4a and Fig. 4b, which implies that the transformation from γ to α is by the massive reaction. However, they have distinctly different microstructural features. The microstructural difference is revealed more clearly in Figs 5a and 5b, which are the microstructures shown by SEM for the specimens held at 810 °C and 830 °C, respectively.

The ε precipitates are not etched by the Nital solution and are shown to be white inside the dark rounded Fe-rich particles in Figs 4a and 4b. These precipitates, which had been formed by the spinodal reaction during cooling, would be initially distributed uniformly. The coarsening kinetics of these precipitates depend on whether the $\gamma \rightarrow \alpha$ transformation took place during isothermal holding or during cool-

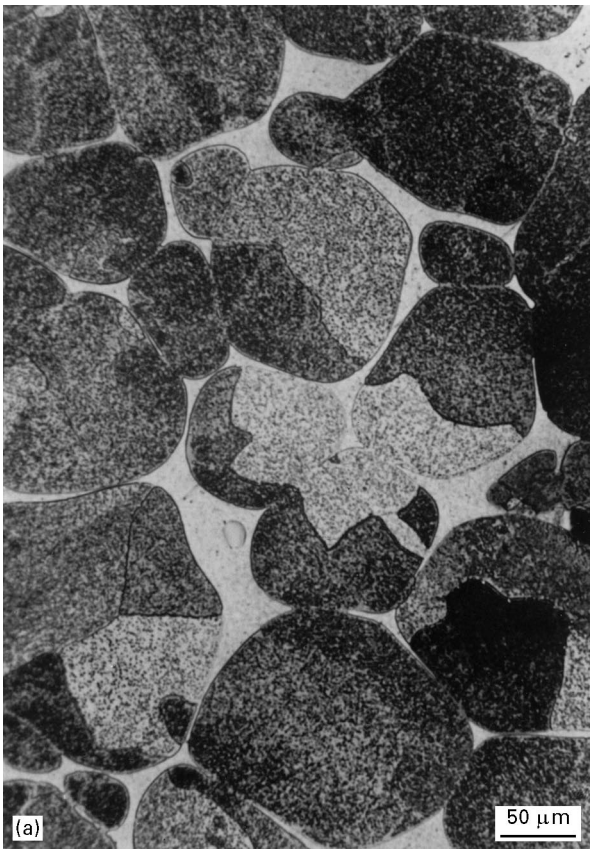

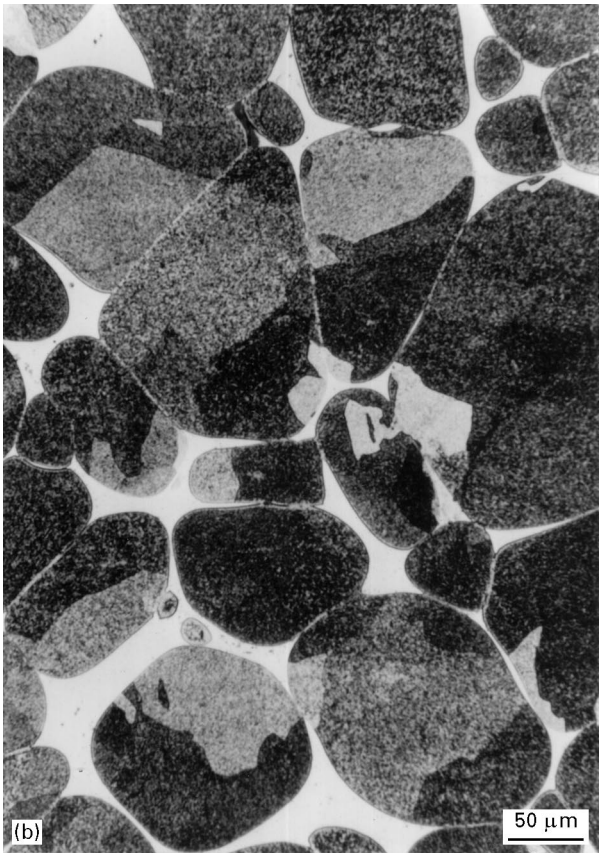

Figure 4 Microstructures of the Fe–20 wt% Cu specimens sintered at 1150 °C for 12 h and then isothermally held for 48 h at (a) 810 °C and (b) 830 °C before being cooled to room temperature.

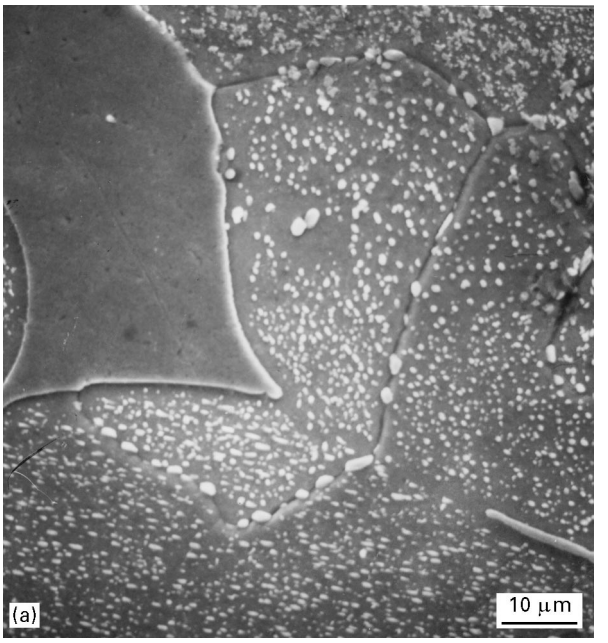

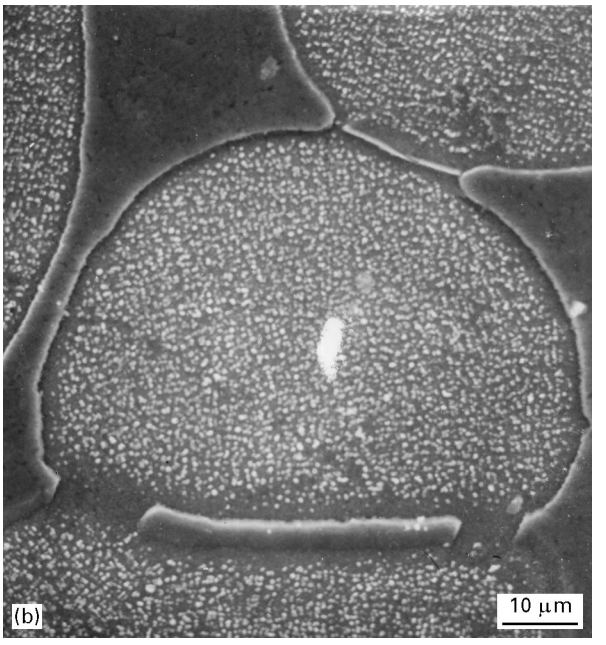

Figure 5 Microstructures shown by SEM of the same specimens as those of Figs 4a and b.

ing after holding. Coarsening of ε will be rapid at the grain boundaries available during holding. The irregular boundaries inside the round Fe-rich particles are the α grain boundaries, which were formed by the $\gamma \rightarrow \alpha$ transformation. The previous γ grain boundary can be located using the dihedral junction between the contacting Fe-rich particles. In Figs 4a and 5a, the dominant coarsening of ε took place along these irregular boundaries, while in Figs 4b and 5b, the dominant coarsening of ε took place along the previous γ grain boundaries. The ε precipitates of Figs 4b and Fig 5b appear to form continuous slabs at the previous γ grain boundaries. The continuous slabs of the precipitates contrasts with the discrete precipitates along the α grain boundaries of Figs 4a and 5a. This difference might be related to the difference between ε–γ and ε–α interfacial energies. The continuous slabs of the ε precipitates along the γ grain boundaries imply that the ε/γ interfacial energy is less than half the grain-boundary energy of γ. Since both ε and γ phases have the same crystal structure, the interfacial energy between them is expected to be relatively low.

These results indicate that the α grain boundaries were formed in the early stage of the holding in the specimen of Figs 4a and 5a while they were not in the specimen of Figs 4b and 5b. These results agree with our expectation that the composition-invariant $\gamma \rightarrow \alpha$ transformation will take place during holding at 810 °C and will not during isothermal holding at 830 °C. The untransformed γ during holding at 830 °C will be eventually transformed to α by the composition-invariant mode during cooling after holding, forming the irregular α grain boundaries in Fig. 4b.

Because the contrast is negligible between the α grains in the SEM microstructures, the α grain boundaries should be identified by the other means. In Fig. 5a, they are easily identified because the large ε precipitates exist along them and they are grooved by the relatively deep etching by the Nital solution. The deep etching seems to be related to the copper deficiency along the α grain boundary by the dominant coarsening of ε precipitates. In Fig. 5b, the etching along the α grain boundaries is not so deep as to be easily identified. This different etching behaviour is also revealed in Figs 4a and b. In Fig. 4a, the α grain boundaries appear as the thick boundaries while, in Fig. 4b, they are revealed mainly by the contrast between the α grains.

Another microstructural difference is the size of the ε precipitates. The size of the ε precipitates in Fig. 5a is much larger than that in Fig. 5b although the magnification (1900 ×) of Fig. 5a is smaller than that (2850 ×) of Fig. 5b. Allso, the holding temperature of Fig. 5a is 20 °C lower than that of Fig. 5b. The diffusivity in α is about two orders of magnitude higher than in γ at these temperatures. These results further indicate that coarsening of ε precipitates took place in the α matrix for the specimen of Fig. 5a and it took place in the γ matrix for the specimen of Fig. 5b.

3.3. Discontinuous eutectoid decomposition

Figs 4 and 5 agree with our expectation that the isothermal composition-invariant $\gamma \rightarrow \alpha$ transformation would take place if the composition of γ shifts to the Fe-rich region of the line aA in Fig. 2. For the specimen held at 830 °C, the composition of γ cannot fall into the metastable α one-phase region. Thus, during holding at 830 °C, the only way that the γ phase can transform to α would be by the long-range diffusion accompanying the composition change. We observed that this mode of transformation had taken place in some part of the specimen held at 830 °C for 48 h. The ε precipitates which are much larger than even those along the grain boundaries in Fig. 5a are observed in some part of the Fe-rich particles for the specimen held at 830 °C for 48 h. The part showing such microstructures is less than 10% of the specimen.

The OM and SEM microstructures are shown in Figs 6a and b respectively, where both coarse and fine ε precipitates are distinctly divided by the straight boundary. The fine precipitates are the same as shown in Fig. 5b. We concluded that these coarse ε precipitates were produced by the long-range diffusion at the phase boundaries accompanying the composition change. The distinct division between the fine and the coarse precipitates indicates that the transformation is the discontinuous reaction, although it is a non-lamella type. This reaction would correspond to the eutectoid decomposition into the equilibrium α and ε.

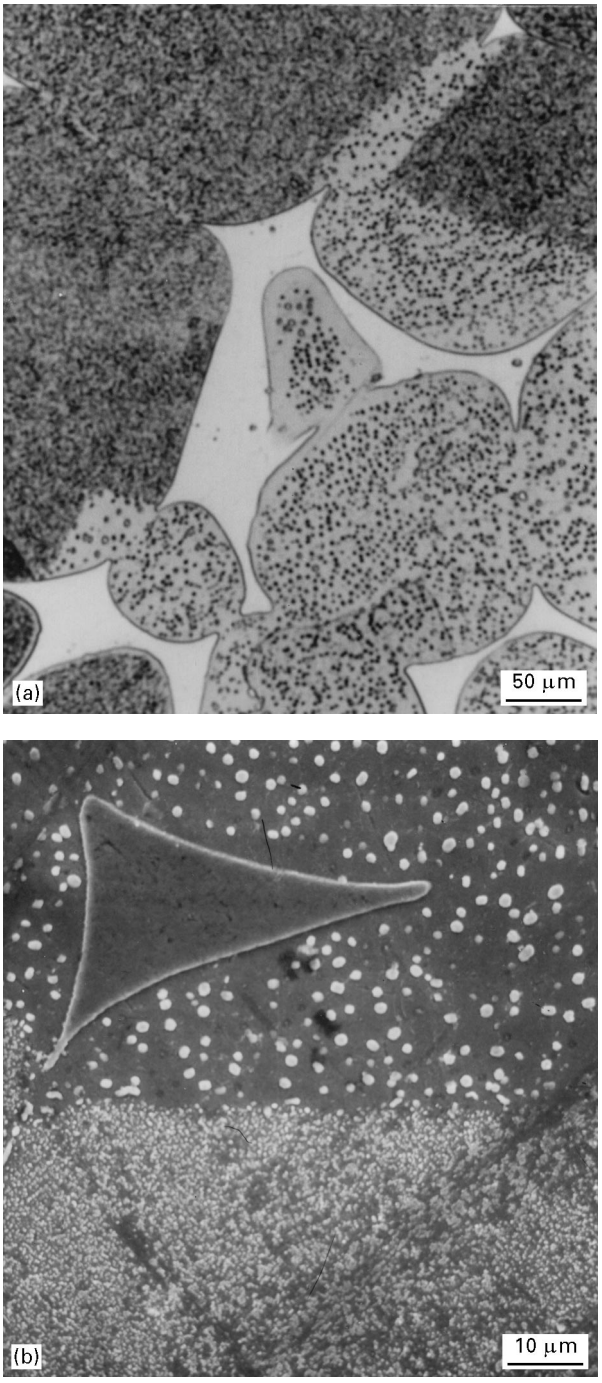

Figure 6 Microstructures determined by (a) OM and (b) SEM of the part showing very large ε precipitates in the specimen of Fig. 5b.

This reaction seems to be extremely slow because less than 10% of the reaction has completed after holding for 48 h at 830 °C. Since the supersaturation of copper in the γ matrix is expected to come mainly from the strain energy and the capillarity of the ε precipitates, the decomposition of γ into the equilibrium α and ε should be achieved by coarsening of the ε precipitates. The boundaries between the coarse and the fine precipitates tended to be straight as shown in Figs 6a and b, which is in contrast with the irregular

boundaries in Figs 4 and 5. The straight boundary indicates that the growth velocity, which is related to the diffusivity and the driving force, depends on the orientation between the growing α and the retreating γ.

3.4. Differential thermal analysis of the isothermal transformation

The isothermal $\gamma \rightarrow \alpha$ transformation was further studied by DTA. The Fe–10 wt% Cu compacts were heated to 1150 °C and held for 3 h for homogenization of copper in the Fe-rich γ solid solution. Three specimens were cooled from 1150 to 830 °C, 810 °C and 800 °C, respectively, and isothermally held for 10–12 h before cooling to room temperature. The alumina powder was used as the standard in the DTA experiment. Because of the difference between the heat capacities of the standard and the specimen, pseudo-endothermic or pseudo-exothermic peaks arise when the temperature is changed abruptly.

Figs 7a, b and c are the DTA curves of temperature difference versus time for the specimens isothermally held at 830 °C, 810 °C and 800 °C, respectively. In Fig. 7, the large pseudo-endothermic hump appears at a time of about 300 min. This hump arises from the cooling from the sintering temperature to the isothermal holding temperature. Within this hump, two sharp peaks are observed; the first is caused by the solidification of the Cu-rich solid and the second by the spinodal precipitation of ε during cooling. The temperatures at which these transformations took place were confirmed by the DTA curves of temperature difference versus temperature, which are not shown in this paper.

Isothermal holding starts at a time of about 350 minutes. In Fig. 7a, the specimen was held for 10 h at 830 °C and no peaks are observed during holding but, at the time of about 950 min, which corresponds to the end of holding, two exthothermic peaks are observed: the first one is large and the second small. The first peak corresponds to the $\gamma \rightarrow \alpha$ transformation and the second peak to the magnetic transition which occurred during cooling. The first peak appeared at about 790 °C and the second at about 760 °C in the DTA curves of temperature difference versus temperature. The magnetic transition in the Fe–Cu system is reported to take place at 760 °C [11]. This result indicates that the $\gamma \rightarrow \alpha$ did not take place during holding for 10 h at 830 °C and that the transformation took place during cooling after holding.

In Fig. 7b, the specimen was held for 10 h at 810 °C and at the start of holding a very shallow broad exothermic peak is observed. The peak starts from about 350 min and ends at about 600 min. After holding, only one exothermic peak appears at the time of about 950 min. This peak appears at 760 °C in the curves of temperature difference versus temperature and corresponds to the magnetic transition. Thus, the shallow broad peak starting from about 350 min and ending at about 600 min should represent the $\gamma \rightarrow \alpha$ transformation. This result implies that the composition-invariant isothermal $\gamma \rightarrow \alpha$ transformation took

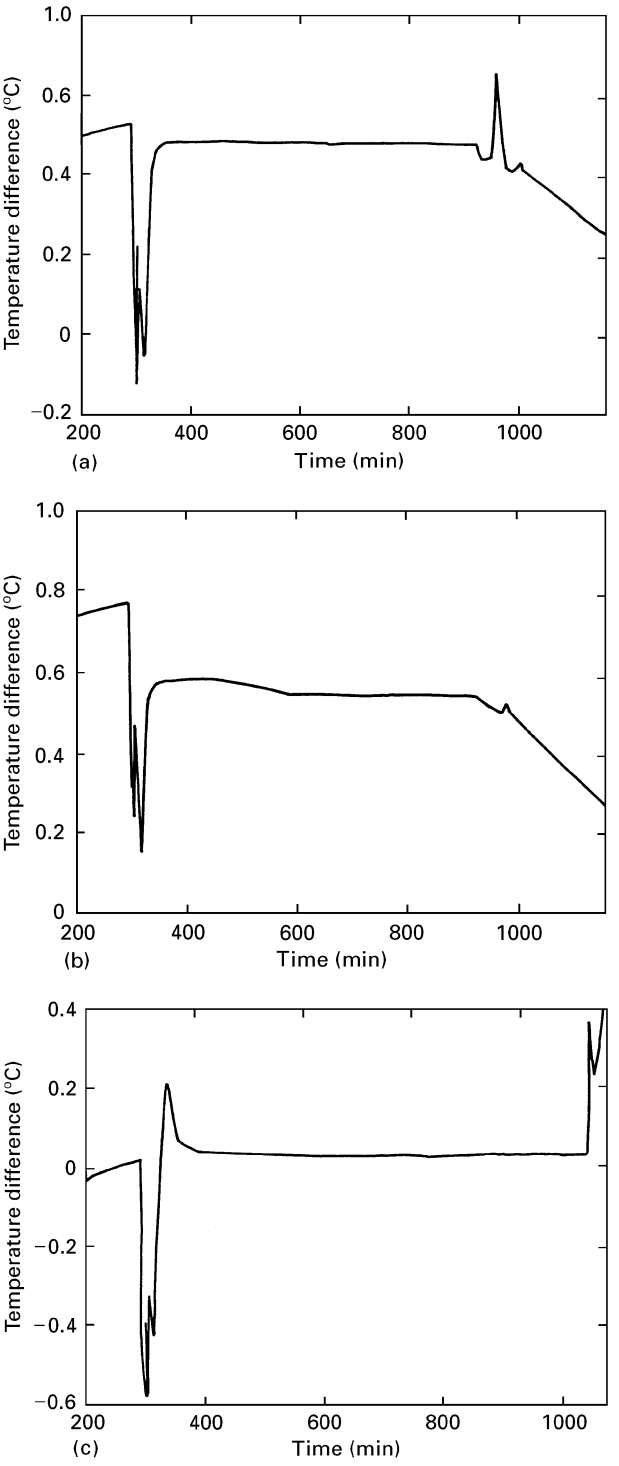

Figure 7 DTA curves for the Fe–10 wt% Cu specimens isothermally held at (a) 830 °C, (b) 810 °C and (c) 800 °C.

place over the time interval of about 250 min. The reason that the isothermal $\gamma \rightarrow \alpha$ transformation did not take place abruptly but took place over some time interval can be understood by considering that the change is the composition of γ into the metastable α one-phase region is achieved by the further precipitation of ε.

In Fig. 7(c), the specimen was held for 12 h at 800 °C and, at the start of holding, the large sharp exothermic peak appears. The peak starts from about 350 min and ends at about 400 min. After holding, only one exothermic peak appears at the approximate time of

1070 min. This peak appears at 760 °C in the DTA curve of temperature difference versus temperature curve and corresponds to the magnetic transition. Compared with the specimen held at 810 °C, the isothermal $\gamma \rightarrow \alpha$ transformation took place over a relatively short time interval. This behaviour can be understood by considering the shape of the line of aA in Fig. 2. The line of aA contains a higher concentration of copper at 800 ° than at 810 °C. Thus, the composition of γ will change into the metastable α one-phase region over a much shorter time interval at 800 °C than at 810 °C.

3.5. Cooling rate required for massive transformation

If the massive transformation is defined as the thermally activated and composition-invariant transition, supercooling of the high-temperature phase into the single-phase region of the low-temperature phase would be a sufficient condition for the massive transformation to operate as long as the supercooled temperature is high enough. This does not mean that supercooling into a single-phase region is a necessary condition. We believe that the composition-invariant and thermally activated transition is possible in the two-phase region when the cooling rate is fast. All the thermally activated allotropic and polymorphic transitions should be classified as the massive transformation. Recently, we showed that the typical microstructure of the massive transformation was developed in pure Fe cooled at $1\,^{\circ}C\,s^{-1}$ [10], which is much lower than specified previously based on the "three-zone behaviour" [4]. It should be noted that in the previous reports [15, 16], the cooling rate for the massive transformation of the Fe–Cu alloy was specified to be higher than $1000\,^{\circ}C\,s^{-1}$ also based on the "three-zone behaviour". The classification of the massive transformation by the three-zone behaviour does not seem to be valid. The possible explanation for the origin of the three-zone behaviour will be given in the next section.

The previous statement by Phillips [1] that the cooling rate for the massive transformation must be fast enough to suppress any composition change cannot be generalized to all systems, although it maybe nearly true for the Cu–Zn system. Phillips observed that the occurrence of the massive transformation in the Cu–Zn system was very sensitive to the composition. In a Cu–37.3 at% Zn alloy, which can fall into the α one- phase region during cooling, the $\beta \rightarrow \alpha$ reaction took place dominantly by the massive mode whereas, at compositions greater than 38.3 at% Zn, which cannot fall into the α one-phase region, most β did not transform to α after cooling. The phase diagram of the Cu–Zn alloy has retrograde solubility with a steep solvus line so that, if the Cu–37.3 at% Zn alloy is not cooled fast enough to suppress the composition change, the equilibrium α can precipitate by long-range diffusion and change the composition of the remaining β matrix so that it becomes Zn rich with respect to Cu–38.3 at% Zn. As a result, the remaining β cannot fall into the α one-phase region during cooling and the $\beta \rightarrow \alpha$ transformation is not necessarily composition invariant.

Another system requiring the high cooling rate is an Fe–C alloy, for which the diffusivity of the interstitial carbon atom is very high and the pearlitic reaction is relatively fast. However, in Fe binary alloys having a γ loop in the phase diagram, such as Fe–Cr, Fe–Si and Fe–Mo, very slow cooling would not complete the transformation from γ to α before being cooled into the α single-phase region. It should be noted that in the Fe–Cr system a previously specified high cooling rate of greater than $5000\,^{\circ}C\,min^{-1}$ [4] was questioned because the boundary crossing was observed at a far slower cooling rate [17]. In systems having a congruent maximum or minimum, the slowest cooling of the specimen having the congruent composition would induce the massive transformation because the thermodynamic situation is the same as that of the polymorphic change.

The Fe–Cu system in this paper is an extreme case where the massive transformation from γ to α takes place during isothermal holding initially in the $\gamma + \alpha$ phase region because the continuous precipitation of ε shifts the composition of γ into the metastable α one-phase region.

3.6. Three-zone behaviour

Bibby and Parr [8] and Swanson and Parr [9] reported, for pure Fe and Fe alloys, three different behaviours of the $\gamma \rightarrow \alpha$ transition temperature with the cooling rate: for a cooling rate below $5000\,^{\circ}C\,s^{-1}$, thermal arrest decreases with increasing cooling rate; at a higher rate, it is insensitive to the cooling rate (the upper plateau); at a still higher rate, it becomes lower but is also insensitive to the cooling rate (the lower plateau). On the basis of this three-zone behaviour, Massalski [4, 5] suggested classification into oriented nucleation and growth, a massive reaction and a martensitic transformation. This three-zone behaviour was also observed in the non-ferrous alloys such as Ag–Al [18], Cu–Ga [19] and Pu–Zr [20]. Later, the classification by the three-zone behaviour was questioned by Bhattacharyya, *et al.* [7]. They pointed out that the meaningful relation between the transformation temperature and the cooling rate should be obtained using a logarithmic scale of the cooling rate. By using the logarithmic scale, they found no plateau between the transformation temperature and the cooling rate. Hillert [21] pointed out that the equiaxed ferrite in the Fe-based alloys, which had been regarded as a product of an equilibrium reaction [4], would be a product of a massive transformation. He [6] also questioned the nature of the massive plateau. However, this three-zone behaviour is often quoted in the text books [22, 23] as a standard classification of a massive transformation in relation to other transformations.

Our previous results [10] and present data clearly show that oriented nucleation and growth is not obtained from extreme slow cooling nor from isothermal holding. The possibility about the origin of the three-zone behaviour is worth mentioning. In the polycrys-

talline microstructure, there are four geometrically different nucleation sites, which are, in the order of increasing nucleation barrier, four-grain corner, three-grain edge, two-grain face and matrix [24]. Because of the nature of the nucleation rate, which tends to be zero below a certain amount of undercooling and increases abruptly to very high values above that, there exists critical undercooling for onset of a given type of the nucleation [25]. Although four-grain corners have the lowest nucleation barrier, they have the smallest nucleation sites per unit volume. Christian [25] calculated that, for a grain size of 0.1 mm, the ratio of grain to corner is $10^{18}:1$.

When the undercooling is small, the ratio of the nucleation rate at the site of the lower nucleation barrier to that of the higher nucleation barrier is so large that the overall contribution in nucleation would be dominant at the site having a low nucleation barrier such as the four grain corner. When the undercooling is very large, the ratio of the nucleation rate of the sites having a lower nucleation barrier to those having a higher nucleation barrier approaches unity. In this case, nucleation will be dominant in the site having the highest nucleation sites per unit volume such as matrix.

The increasing cooling rate would be equivalent to increasing undercooling and, with increasing cooling rate, the site of dominant nucleation changes from four-grain corners to three-grain edges or two-grain faces in the range of relatively slow cooling. Thus, the thermal arrest temperature is expected to decrease with increasing cooling rate. When the cooling rate is high enough to exceed the critical undercooling for the nucleation in the matrix, the nucleation rate would be so high that further increase in the cooling rate could not suppress nucleation in the matrix because of the avalanche nature of the nucleation rate. This would make thermal arrest relatively insensitive to the cooling rate, leading to the first plateau in the three-zone behaviour. When the cooling rate increases still further, the second plateau, which corresponds to the martensitic reaction, will appear. Previously, Caretti and Bertorello [26] reported the experimental results, showing this possibility for the three-zone behaviour.

4. Conclusions

Typical microstructural features of the massive transformation were observed in the Fe–Cu alloys, which were cooled at $0.1\,^{\circ}C\,s^{-1}$ or isothermally held at 810 °C. The thermal arrest for the isothermal $\gamma \rightarrow \alpha$ transformation was also confirmed by DTA. If this $\gamma \rightarrow \alpha$ transformation is classified as the massive reaction, the supercooling into the single-phase region might be a sufficient condition for the massive transformation as long as the supercooled temperature is high enough to allow the atomic jumps across the interphase boundary. In some substitutional alloys, the cooling rate for the massive transformation to operate is expected to be much lower than specified before.

Acknowledgements

Fruitful discussions with Professor Hillert and Professor Ågren at Royal Institute of Technology in Sweden are greatly appreciated. This work was supported by the Korea Ministry of Science and Technology and the Korea Science and Engineering Foundation through the Center for Interface Science and Engineering of Materials.

References

1. A. J. PHILLIPS, *Trans. Metall. Ser. AIME* **89** (1930) 194.
2. T. B. MASSALSKI, *Acta Metall.* **6** (1958) 243.
3. J. E. KITTL and T. B. MASSALSKI, *ibid.* **15** (1967) 161.
4. T. B. MASSALSKI, "Phase Transformations" (American Society for Metals, Metals Park, OH, 1970) p. 454.
5. *Idem., Metall. Trans. A* **15** (1984) 421.
6. M. HILLERT, *ibid.* **15** (1984) 411.
7. S. K. BHATTACHARYYA, J. H. PEREPEZKO and T. B. MASSALSKI, *Scripta Metall.* **7** (1973) 485.
8. M. J. BIBBY and J. G. PARR, *J. Iron Steel Inst. London* **202** (1964) 100.
9. W. D. SWANSON and J. G. PARR, *ibid.* **202** (1964) 104.
10. N. M. HWANG, C. Y. YOO and D. Y. YOON, in "Solid → Solid Phase Transformations", edited by W. C. Johnson, J.M. Howe, D. E. Laughlin and W. A. Soffa (Minerals, Metals and Materials Soc., New York, 1994) p. 511.
11. T. B. MASSALSKI, "Binary Alloy Phase Diagrams" (2nd Edn, American Society for Metals, Metals Park, OH, 1990) p. 1408.
12. J. J. URCOLA-GALARAZ and M. FUENTES-PERES, *Metallography* **12** (1979) 125.
13. A. HULTGREN, A. JOSEFSSON, E. KULA and G. LAGERBERG, *Jernkontorets Ann.* **142** (1958) 165.
14. O. KUBASCHEWSKI, J. F. SMITH and D. M. BAILEY, *Z. Metallkde* **68** (1977) 495.
15. E. RÄSÄNEN, *Scand. J. Metall.* **2** (1973) 257.
16. J. FAUSTMANN and C. PARACIOS, *Rev. Metall.* **14** (1978) 133.
17. T. B. MASSALSKI, S. K. BHATTACHARYYA and J. H. PEREPEZKO, *Metall. Trans. A* **9** (1978) 53.
18. E. B. HAWBOLT and T. B. MASSALSKI, *ibid.* **2** (1971) 1771.
19. J. E. KITTL and C. RODRIGUEZ, *Acta Metall.* **17** (1969) 925.
20. A. J. PERKINS, A. GOLDBERG and T. B. MASSALSKI, *J. Nucl. Mater.* **41** (1971) 39.
21. M. HILLERT, *Metall. Trans. A* **6** (1975) 5.
22. D. A. PORTER and K. E. EASTERING, "Phase Transformations in Metals and Alloys" (Van Nostrand, London, 1981) p. 357.
23. A. K. JENA and M. C. CHATURBEDI, "Phase Transformations in Materials" (Prentice Hall, Englewood Cliffs, NJ, 1992) p. 256.
24. J. W. CAHN, *Acta Metall.* **4** (1956) 449.
25. J. W. CHRISTIAN, "The Theory of Transformation in Metals and Alloys (Pergamon, London, 1975) p. 455.
26. J. C. CARETTI and H. R. BERTORELLO, *Acta Metall.* **31** (1983) 325.

Received 24 June 1996
and accepted 10 March 1997